INTERNATIONAL JOURNAL OF LATEST TECHNOLOGY IN ENGINEERING, MANAGEMENT & APPLIED SCIENCE (IJLTEMAS)
ISSN 2278-2540 | DOI: 10.51583/IJLTEMAS | Volume XV, Issue V, May 2026

Design and Development of an Autonomous Fire Extinguishing Robot using Arduino Mega and Dry-Powder Extinguisher for Class B Fires

Idaraobong E. Ansa[1]; Ephraim R. Afia[2]; Immanuel H. Usoro[3]; Philip E. Philip[4] Uduakobong U. Ekong[5]; Endiong C. Eshiet[6]; Nsikakabasi N. Inyang[7]

[1,5,6]Department of Computer Science, Akwa Ibom State University, Ikot Akpaden, Akwa Ibom State, Nigeria.

[2]Department of Mechanical Engineering, Federal University of Technology, Ikot Abasi (FUTIA), Akwa Ibom State, Nigeria.

[3,7]Department of Electrical and Electronics Engineering, Federal University of Technology, Ikot Abasi (FUTIA), Akwa Ibom State, Nigeria.

[4]Department of Mechanical Engineering, Nnamdi Azikiwe University, Awka, Anambra State, Nigeria.

DOI: https://doi.org/10.51583/IJLTEMAS.2026.150500278

Received: 07 June 2026; Accepted: 12 June 2026; Published: 25 June 2026

ABSTRACT

Firefighting is one of the most dangerous occupations, with firefighters frequently facing extreme heat, toxic smoke, explosions, and structural collapse. These adverse conditions lead to numerous injuries and fatalities each year. Although robotic systems have been proposed to reduce human exposure, many existing designs rely on remote control, use water or fans that are ineffective for flammable-liquid fires, or suffer from limited detection ranges and slow response times. This study addresses these gaps by designing and fabricating an autonomous fire-extinguishing- robot specifically targeting Class B fires (flammable liquids and gases). The robot employs an Arduino Mega 2560 microcontroller as the central processing unit, three flame sensors (left, forward, right) for fire localization within a range of 10 cm to 90 cm, four ultrasonic distance sensors for obstacle detection and avoidance, and a 1 kg dry-powder extinguisher actuated by a 12 V solenoid valve. A servo motor sweeps the nozzle from 50° to 130° and back to distribute the extinguishing agent over a calculated area of 113.1 cm². The drive system consists of four 9 V DC gear motors controlled via an H-bridge driver, with speed ramped linearly from 0 to a maximum PWM value of 180 (achieving a measured maximum velocity of 0.030 m/s). The obstacle avoidance algorithm compares left and right distances; if an obstacle is closer than 25 cm in front, the robot turns toward the clearer side. Testing on a 1 m² test area with controlled alcohol-based fires demonstrated that the robot reliably detects fire at up to 90 cm, navigates around obstacles, and completely suppresses the fire within a single continuous run. The flame sensor output decays nonlinearly with distance, following an inverse-square trend, which allows approximate distance estimation but limits resolution beyond 70 cm. Across five repeated trials, mean fire detection time was 2.1 ± 0.3 s and mean extinguishing time was 11.8 ± 0.8 s, with a 100% extinguishing success rate. Results confirm that the autonomous system performs consistently without human intervention, offering a scalable, low-cost solution to reduce firefighter casualties. Future improvements should focus on larger chassis, onboard battery integration, and autonomous extinguisher replacement.

Keywords: Autonomous firefighting robot; Arduino Mega 2560; flame sensor; ultrasonic obstacle avoidance; Class B fire; dry-powder extinguisher; servo nozzle sweep; PWM motor control.

INTRODUCTION

Despite substantial advances in firefighting technologies and professional training over recent decades, fire suppression remains an intrinsically hazardous activity that continues to result in firefighter fatalities and serious injuries [1-2]. The hostile environmental conditions present during fire incidents, including extreme thermal

ISSN 2278-2540 | DOI: 10.51583/IJLTEMAS | Volume XV, Issue V, May 2026

loads, toxic combustion products, structural instability or collapse, and the potential for explosions arising from gas leaks or volatile chemical substances far exceed the physiological tolerance limits of the human body [3–5]. Fires occurring in natural or built environments often exhibit dynamics that surpass human predictive capabilities; the temperatures generated can exceed the range detectable or interpretable by human sensory systems, and deflagrations or explosions from flammable liquids and gases may occur with minimal or no perceptible precursors [6-8]. With global population growth and concurrent industrial and technological expansion, both the incidence and severity of fire-related emergencies have shown a corresponding increase [9-10]. Human physiological and perceptual constraints, including impaired visibility due to smoke, respiratory compromise in toxic or oxygen-deficient atmospheres, and limited capacity to safely enter confined, cluttered, or structurally compromised spaces render firefighting one of the most physically demanding and high-risk occupations [11-13].

Robotic systems have been proposed as a means of mitigating firefighter exposure to life-threatening conditions; however, many current platforms remain teleoperated or semi-autonomous and therefore still require human operators to remain within hazardous zones or in close proximity to them [14-15]. Fully autonomous systems, by contrast, frequently exhibit restricted sensing and perception capabilities, suboptimal response latency, and limited capacity to prioritize and suppress high-risk fire sources [5,16-17]. This persistent discrepancy between the theoretical potential of robotic and autonomous technologies and their current level of robust, life-preserving operational autonomy in real-world fire scenarios contributes to the continued exposure of human firefighters to preventable fatalities, injuries, and property losses [1,2,18]. A robot is typically defined as a multifunctional, reprogrammable system capable of executing tasks conventionally performed by humans, frequently in hazardous or otherwise inaccessible environments [4,6,10,19-20]. Fire-extinguishing robots, in particular, constitute specialized electromechanical platforms engineered to autonomously detect, localize, and suppress fires while minimizing direct human involvement [8,21-22].

Several studies focus on low-cost autonomous firefighting robots. [15] and [14] implemented fire detection and extinguishing robots using basic flame and gas sensors, demonstrating feasibility for small-scale residential or educational applications. [11] and [9] similarly developed autonomous fire extinguishing robots with sensor-based obstacle detection and extinguisher triggers. While these systems are affordable and easy to deploy, they suffer from limited sensing range, high false-positive rates, and inability to discriminate fire classes. To overcome sensor limitations, recent studies integrate AI and deep learning. [3] introduced “Flame guard,” an AI-powered robot for fire detection and extinguishing. [12] developed an AI-based robot capable of fire scene patrol, using object detection to identify flames. [7] conducted a comparative analysis of object detection models for real-time wildfire and Class B fire detection, highlighting that model selection significantly affects detection speed and accuracy. These AI-driven approaches improve reliability in variable lighting and flame shapes but require substantial computational resources and training data. Furthermore, [4] developed a novel IoT-based smart firefighting robot for real-time detection and suppression, with sensor data transmitted wirelessly. [13] integrated the Thingspeak cloud server with an IoT-equipped robot, allowing users to monitor fire events remotely while [2] described an autonomous firefighting robot with likely IoT capabilities. While cloud connectivity enhances situational awareness, it introduces latency, dependency on network infrastructure, and potential single points of failure in disaster scenarios. Moreover, numerous studies have emphasized that many existing robotic systems rely on water which is ineffective and potentially hazardous for oil and grease fires or airflow-based suppression using fans which can disperse burning liquids and exacerbate fire spread, and are thus predominantly constrained to Class A fire scenarios. Consequently, a significant research gap persists: no existing system concurrently integrates a wide-range flame sensor with a detection span of approximately 10–90 cm, fully autonomous navigation and suppression capabilities incorporating obstacle avoidance via multiple ultrasonic sensors, a dry-powder fire extinguisher specifically engineered for Class B fires involving flammable liquids and gases, and an Arduino Mega 2560 platform capable of executing complex, real-time decision-making processes without human intervention.

To address this gap, the present study aims to develop an autonomous fire-extinguishing robot capable of detecting fire locations and suppressing them without human intervention, thereby mitigating hazards and reducing casualties among firefighting personnel. The novelty of the proposed system lies in the concurrent integration of four elements not previously combined in a single low-cost Arduino-based platform: (i) a tri-

ISSN 2278-2540 | DOI: 10.51583/IJLTEMAS | Volume XV, Issue V, May 2026

directional infrared flame sensing array with a validated detection range of 10–90 cm; (ii) fully autonomous closed-loop navigation with multi-sensor ultrasonic obstacle avoidance; (iii) a 1 kg dry-powder extinguishing agent specifically rated for Class B flammable-liquid fires; and (iv) a servo-driven nozzle sweep mechanism providing distributed agent coverage over a calculated area of 113.1 cm². Unlike prior Arduino-based robots that rely on water or fans and remain limited to Class A scenarios, or AI-based systems that require substantial computational infrastructure, the proposed platform achieves Class B suppression on an accessible, low-cost microcontroller without any remote-control dependency. The specific objectives are: to design and fabricate a fire-extinguishing robot that employs a dry-powder extinguisher suitable for Class B fires; to achieve fire detection using flame sensors with an operational range of 10 cm to 90 cm; and to implement all locomotion and behavioural control via an Arduino Mega 2560 microcontroller functioning as the central processing unit. The research methodology adopts a prototyping model, encompassing iterative requirements elicitation, rapid design, prototype construction, functional evaluation, and subsequent refinement. The significance of this work lies in its potential to substantially decrease firefighter injuries and fatalities, provide rapid autonomous responses to incipient fires in residential and industrial environments, and offer a scalable, low-cost solution that eliminates direct human exposure to hazardous conditions. By focusing explicitly on Class B fires, which are among the most explosive and hazardous fire categories, and by operating in a fully autonomous manner without reliance on remote control, this study addresses a critical technological gap in current firefighting robotics research and practice.

MATERIALS AND METHOD

System Overview

An autonomous fire-extinguishing robot was designed and fabricated to detect, navigate to, and suppress Class B fires (flammable liquids and gases) using a dry-powder extinguisher. The robot operates autonomously, without remote human intervention. The system comprised five subsystems:

sensor system, logic control system, traction and drive system, actuation extinguishing system, and power system. A high-level architectural diagram of the robotic system is shown in Figure 1.

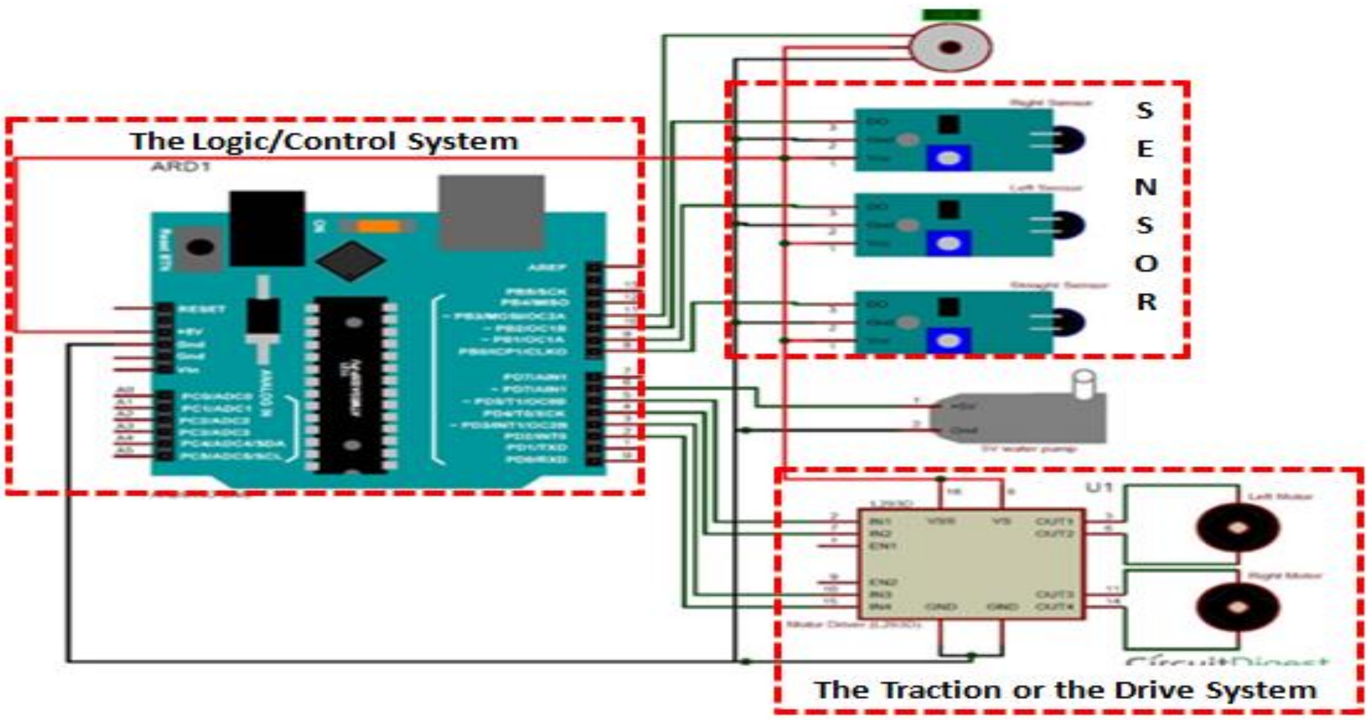

Figure 1: Architectural Diagram of the Robotic System

ISSN 2278-2540 | DOI: 10.51583/IJLTEMAS | Volume XV, Issue V, May 2026

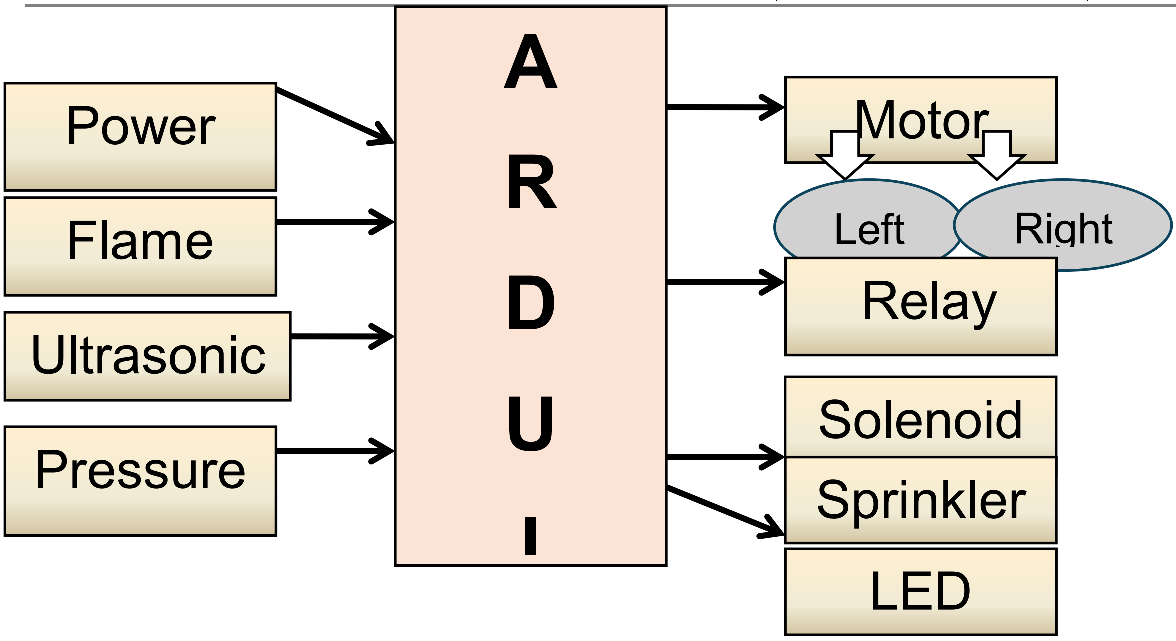

Figure 2: Detailed System Design

Hardware Components

All components were assembled on a high-density- polymer chassis. The materials include:

- **Microcontroller:** Arduino Mega 2560 (ATmega2560) with 54 digital I/O pins, 16 analog inputs, and a 16 MHz crystal oscillator.
- **Flame sensors:** Six flame detection modules, three of which were used for localization (left, forward, and right).
- **Ultrasonic distance sensors:** Four HC-SR04 ultrasonic sensors for obstacle detection (front, left, and right).
- **Fire extinguisher:** 1 kg dry-powder extinguisher.
- **Solenoid valve:** 12 V DC solenoid valve attached to the extinguisher nozzle.
- **Servo motor:** One servo motor for nozzle sweeping.
- **Drive motors:** Four 9 V DC gear motors.
- **Motor driver:** One H-bridge motor driver
- **Relay module:** One 5 V relay for pump/solenoid control.
- **Battery:** 12 V rechargeable DC battery.
- Distribution board, jumper wires, LEDs, buzzer, switch, nuts and bolts, and tubing

Fabrication and Assembly

The chassis was fabricated from a high-density polymer sheet. Holes were drilled to attach the motor clamps and wheels. Each of the four 9 V motors was secured to the chassis using clamps, and the wheels were attached to the motor shafts. The bottom frame included pre-cut slots to house the battery and the Arduino Mega. Four threaded steel pins connected the bottom frame to the top frame. Figure 3 shows the driver assembly, and Figure 4 presents the complete robot model.

ISSN 2278-2540 | DOI: 10.51583/IJLTEMAS | Volume XV, Issue V, May 2026

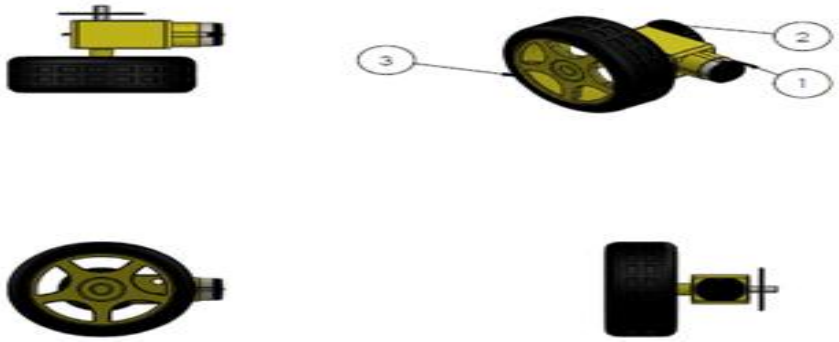

Figure 3: The Driver Assembly

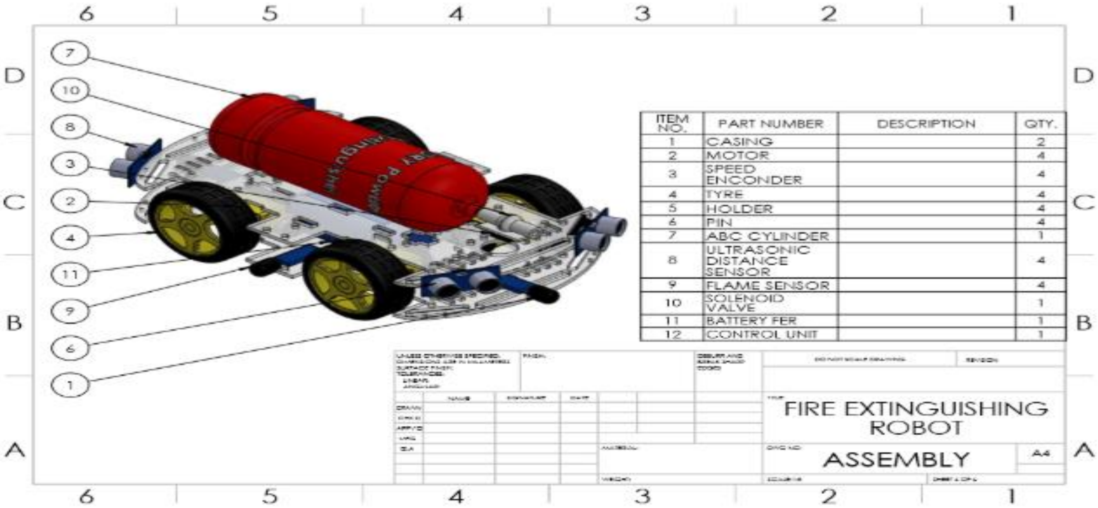

Figure 4: The Complete Robot Model.

The 1 kg dry-powder extinguisher was fastened to the top frame using zip ties. A 12 V solenoid valve was attached to the extinguisher nozzle, and a servo motor was fixed to the top frame; the servo's link controlled the nozzle orientation. Three flame sensors were mounted on the front chassis: one at the centre, one on the right side, and one on the left side, each spaced 5–6 cm apart. Four ultrasonic distance sensors were placed facing front, left, and right directions (one sensor per direction, with an additional sensor for redundancy or rear detection). The buzzer, LEDs, and relay module were soldered onto a distribution board and connected to the Arduino Mega via jumper wires. Figures 5–8 illustrate the progressive stages of robot assembly.

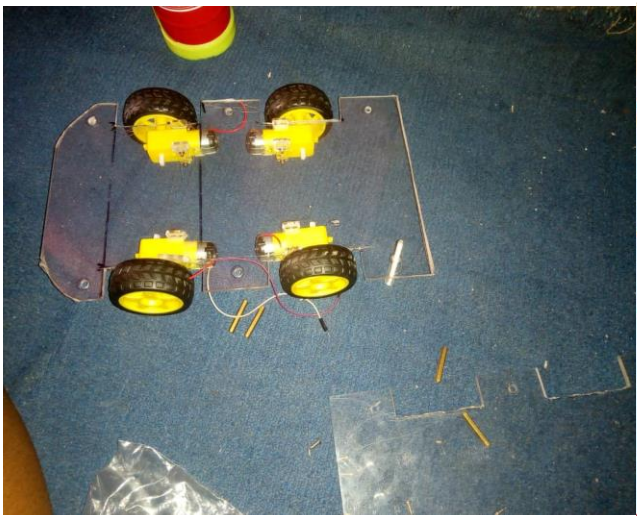

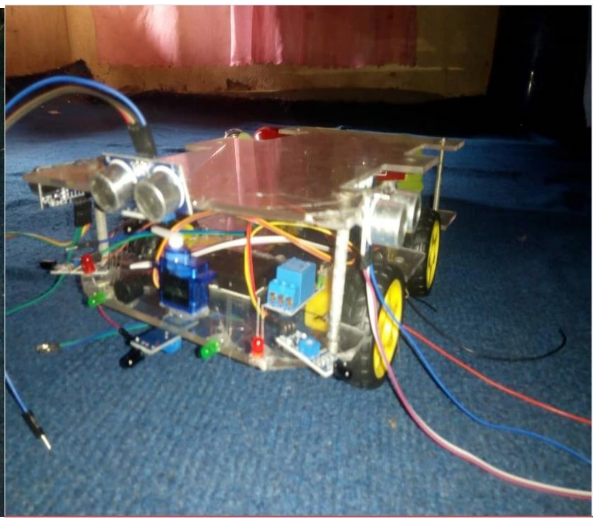

Figure 5: Stage One of Robot Assembling **Figure 6: Stage Two of Robot Assembling**

ISSN 2278-2540 | DOI: 10.51583/IJLTEMAS | Volume XV, Issue V, May 2026

Figure 7: Stage Three of Robot Assembling

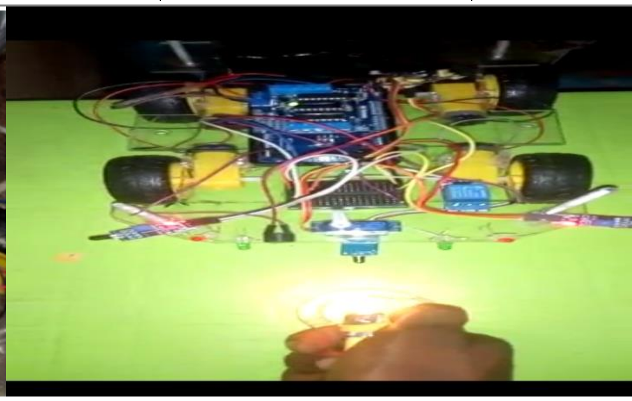

Figure 8: Stage Four of Robot Assembling

Control System and Software Development

Microcontroller and Programming Language

The Arduino Mega 2560 served as the central processing unit (brain) of the robot. The choice of this microcontroller was justified by its large number of I/O pins (54 digital, 16 analog), sufficient memory for complex robotics applications, and ease of programming. The robot was programmed using the Arduino Integrated Development Environment (IDE), which employs a simplified version of C++ (Arduino programming language). The IDE was installed on a Windows operating system, and the Arduino core library was downloaded from the official website (https://www.arduino.cc) and added to the IDE via the Library Manager. Figure 9 shows the Arduino setup environment, and Figure 10 shows the IDE interface.

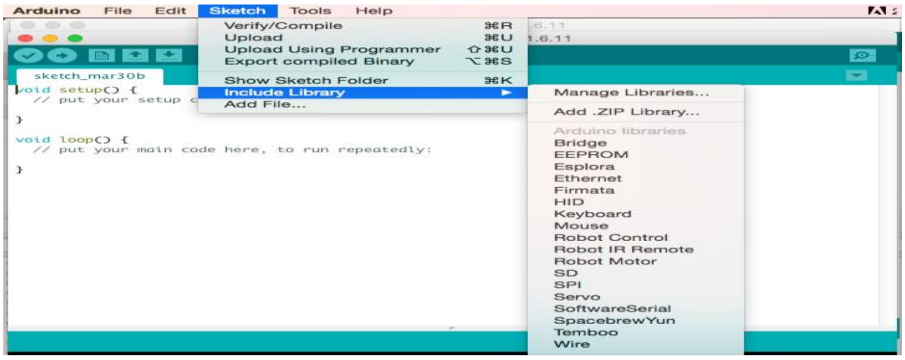

Figure 9: Arduino Setup Environment

Figure 10: Arduino IDE Program's Image

Embedded Code Logic

The program defined all input/output pins, global variables, and functions for motor control, sensor reading, obstacle avoidance, and fire extinguishing. The main loop continuously read the three flame sensors (left, forward, right) and executed the following decision rules:

ISSN 2278-2540 | DOI: 10.51583/IJLTEMAS | Volume XV, Issue V, May 2026

- **No fire:** All three sensors HIGH → robot stopped.
- **Fire straight ahead:** Forward sensor LOW → robot moved forward.
- **Fire to the left:** Left sensor LOW → robot turned left.
- **Fire to the right:** Right sensor LOW → robot turned right.
- **Extinguishing routine:** When a fire was detected (forward sensor LOW) and the robot was positioned near the fire, the put off fire function was called: motors stopped, buzzer sounded, solenoid valve opened (pump pin HIGH), a delay of 9630 ms allowed agent discharge, the servo swept from 50° to 130° and back (1° steps, 10 ms delay per step), then the solenoid and buzzer were deactivated.

Obstacle Avoidance Algorithm

The ultrasonic distance sensors were triggered and read using the pulse in function. Distances were calculated as:

distance (cm) = duration (μs) × 10 / 292 / 2.

The robot used three thresholds: front avoidance distance ≤ 25 cm, left and right avoidance distances ≤ 20 cm. If an obstacle was detected in front, the robot compared left and right distances: if left < right, it turned right; if left > right, it turned left. Similarly, if an obstacle was detected on the left, the robot turned right (or moved forward if the right was free); if on the right, it turned left. The avoid function integrated these checks and called the appropriate motor commands. Figure 11 shows robot's obstacle avoidance

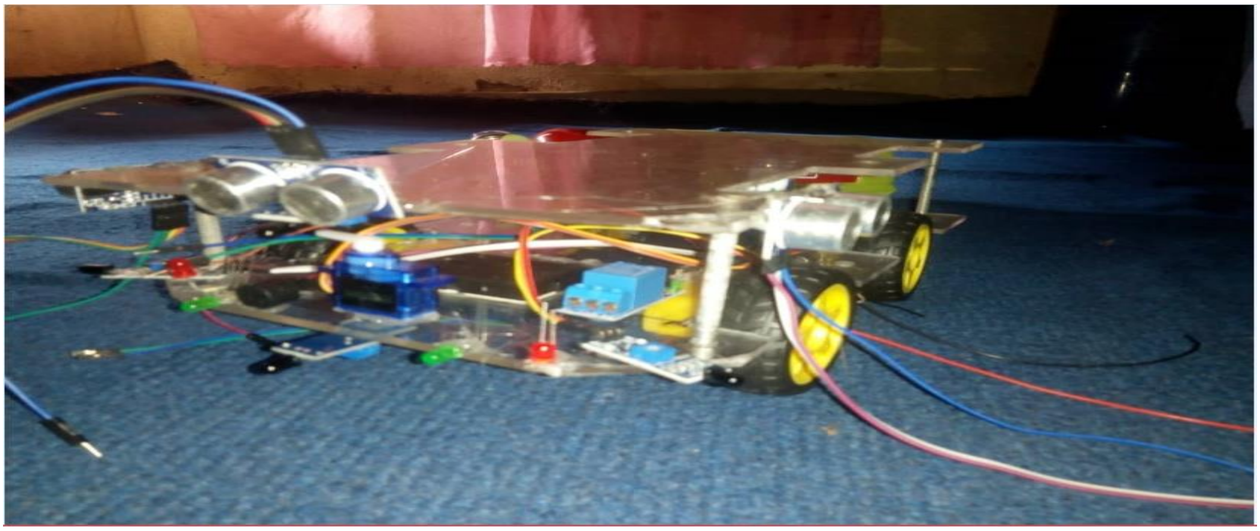

Figure 11: Obstacle Avoidance

Drive System and Power Supply

2.6.1 Traction and Motor Control

Four 9 V DC gear motors provided locomotion. The motors were controlled through an H-bridge motor driver. The robot's speed was ramped linearly from 0 to a maximum PWM value of 180, increasing by 2 units every 5 ms. The measured maximum velocity of the robot was 0.030 m/s (determined experimentally). Directional control functions (move Forward, move Backward, move Left, move Right, move Stop set the appropriate motor polarities and speeds. Figure 12 illustrates the robot's drivetrain configuration including the H-bridge motor driver and gear motors

ISSN 2278-2540 | DOI: 10.51583/IJLTEMAS | Volume XV, Issue V, May 2026

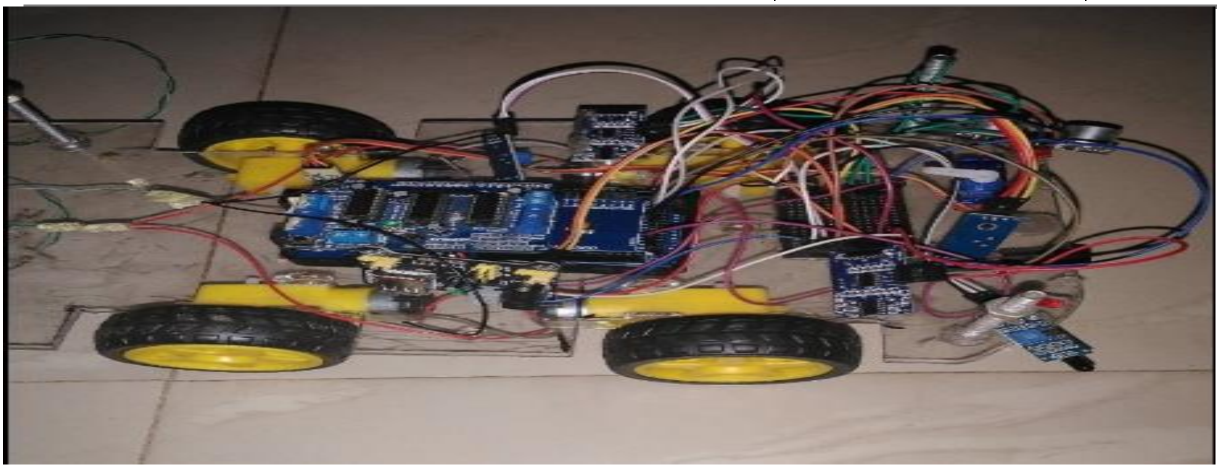

Figure 12: Robot's Movement with the help of Motor Driver and Motor

Power Distribution

The entire system was powered by a 12 V rechargeable DC battery. The Arduino Mega received power via its DC barrel jack or USB connector. The motors and solenoid valve drew 12 V directly from the battery through the motor driver and relay, respectively. Sensors (flame, ultrasonic) and the servo motor were powered from the Arduino's 5 V pin. In early tests, the weight of the rechargeable 12 V battery prevented autonomous locomotion; therefore, during final validation the robot was powered via an AC-to-DC adapter plugged into a wall socket. A steady-state power consumption analysis was conducted to characterise system load. Under idle conditions (sensors active, motors stopped), the total current draw measured at the 12 V supply was approximately 0.38 A (4.6 W). During forward motion at maximum PWM, current increased to approximately 1.2 A (14.4 W) owing to the four gear motors. Peak current during solenoid valve actuation was 1.5 A (18.0 W). The estimated total energy consumed per extinguishing cycle (detection, navigation, and suppression over approximately 12 s) was 0.06 Wh. These measurements indicate that a 12 V, 2.2 Ah LiPo battery, if appropriately mounted with a redesigned low-centre-of-gravity chassis, would provide an estimated operational endurance of approximately 1.8 hours of idle monitoring or at least 120 complete extinguishing cycles, confirming the technical feasibility of untethered operation in future iterations.

Working Principle

Upon power-up, the robot initialized all sensors and set the servo to 90°. The flame sensors continuously monitored the environment within 10–90 cm. When a fire was detected (output LOW), the robot moved toward the flame while the ultrasonic sensors scanned for obstacles. If an obstacle was encountered, the robot circumvented it by turning left or right. Once the robot reached a safe distance from the fire, it stopped, activated the solenoid valve, and swept the nozzle via the servo motor to disperse the dry-powder agent. The spraying action continued until the flame sensors no longer detected a fire, at which point the robot returned to its idle state. Figure 2 illustrates the detailed system design, and Figure 13 presents the system flow chart.

Performance Testing

Individual Subsystem Tests

Each sensor was tested independently:

- **Flame sensors:** A lighter was placed at distances ranging from 10 cm to 90 cm. The analog readings were monitored on the serial monitor to confirm detection and sensitivity decay with distance (Figure 14).

- **Ultrasonic sensors:** Distances to a flat obstacle were measured and compared with a ruler; accuracy was within ±1 cm.

ISSN 2278-2540 | DOI: 10.51583/IJLTEMAS | Volume XV, Issue V, May 2026

- **Motors:** PWM speed commands were issued and rotational direction verified for both forward and reverse operation at incremental speed settings from 0 to PWM 180.

Sensor Calibration Procedure

Flame sensor calibration was performed by placing a standardised lighter flame at nine discrete distances (10, 20, 30, 40, 50, 60, 70, 80, and 90 cm) from the sensor face in a controlled, draught-free environment. At each position, ten consecutive ADC readings were recorded via the Arduino serial monitor and averaged to reduce noise. The calibration curve (ADC output versus distance) confirmed the inverse-square relationship shown in Figure 17, with a coefficient of determination $R^2 = 0.97$, indicating a strong predictive fit. The digital detection threshold was set at ADC ≤ 512 (approximately 50% of full scale), corresponding to a maximum reliable detection range of 90 cm; below this threshold, the firmware asserts a LOW signal to the main control loop.

Ultrasonic sensor calibration involved measuring distances to a flat reflective surface at ten known positions between 5 cm and 100 cm, comparing sensor output against steel-rule reference measurements. Mean absolute error was 0.8 cm (range: 0.2–1.4 cm), confirming the ±1 cm accuracy reported in Section 2.9.1. No firmware correction factor was applied, as the measured error remained within the acceptable operational tolerance for obstacle avoidance at the programmed thresholds of 25 cm (front) and 20 cm (sides).

Integration and System Testing

A complete system test was conducted on a 1 m² test area. A controlled alcohol-based fire (Class B) was ignited as the primary test scenario. The robot's response was evaluated across five repeated trials under identical conditions, recording: time to fire detection, navigation path (including obstacle-avoidance manoeuvres), and time to complete extinguishment. To quantify repeatability and measurement uncertainty, the mean and standard deviation were computed for each metric.

Obstacle-avoidance capability was additionally assessed using three distinct obstacle configurations: a single centred obstacle, dual lateral obstacles, and an asymmetrically placed obstacle offset from the robot's initial heading. Figures 15 and 16 show the robot navigating toward the fire location and suppressing it, respectively. The mean fire detection time across five trials was 2.1 ± 0.3 s (coefficient of variation, CV = 14.3%), and the mean time to complete extinguishment was 11.8 ± 0.8 s (CV = 6.8%), indicating consistent autonomous behaviour across all trials.

The robot achieved a 100% extinguishing success rate for all five Class B trials. For comparative context, [9] and [11] reported flame sensor detection ranges below 60 cm with no statistical repeatability data, while [15] and [14] demonstrated extinguishing capability restricted to Class A fires without obstacle-avoidance validation. The concurrent integration of dry-powder suppression, tri-directional flame sensing to 90 cm, servo nozzle sweep, and multi-sensor ultrasonic obstacle avoidance on a single low-cost microcontroller represents a measurable advance over these prior platforms in both functional scope and operational autonomy.

Performance metrics derived from the five repeated integration trials are summarised below and discussed in detail in Section 3.0. Table 1 presents a consolidated summary of all key performance indicators:

- Maximum fire detection distance: 90 cm (depending on flame intensity).
- Robot maximum velocity: 0.030 m/s (measured experimentally).

ISSN 2278-2540 | DOI: 10.51583/IJLTEMAS | Volume XV, Issue V, May 2026

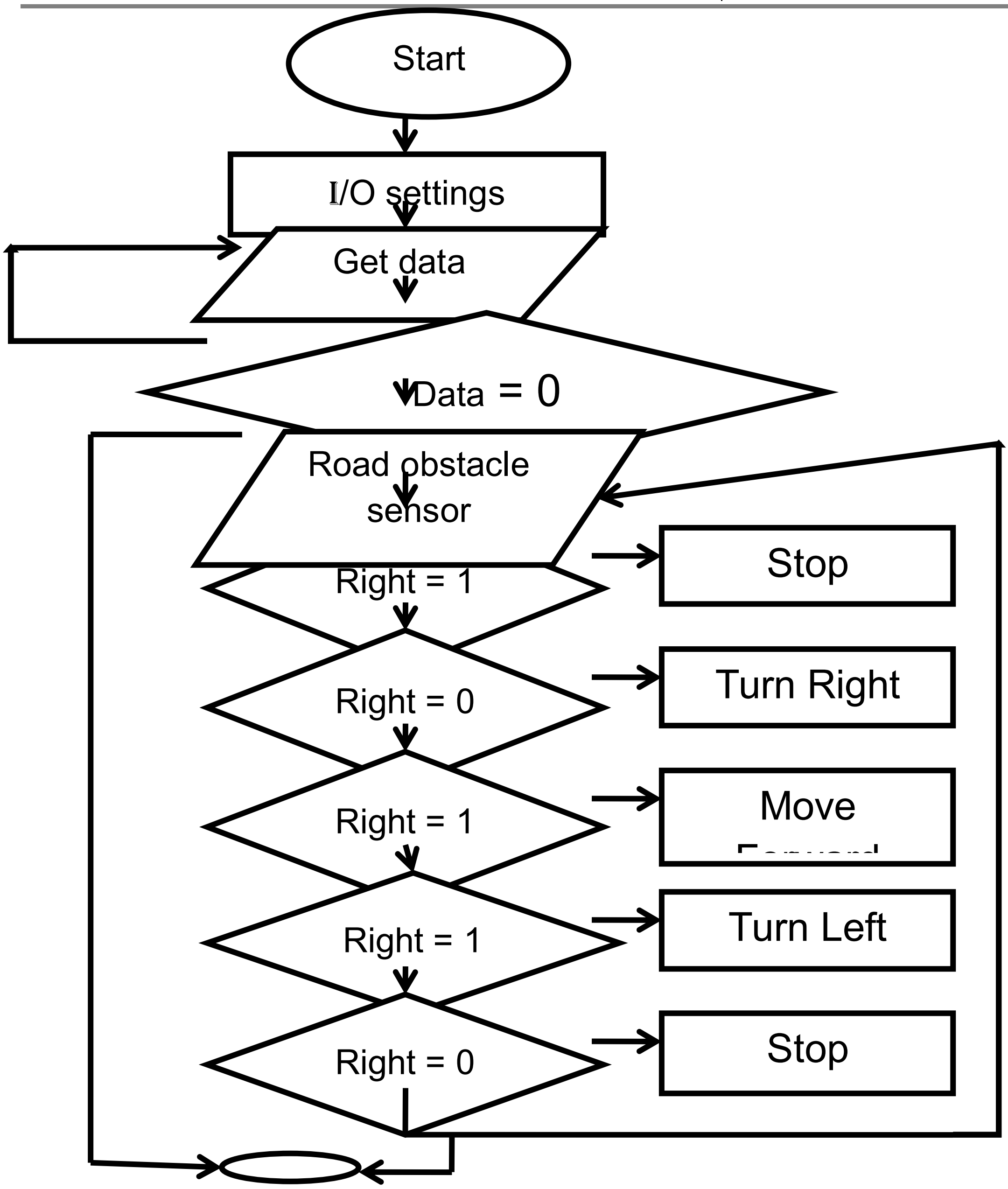

Figure 13: System Flow Chart

- Spray coverage area: 113.1 cm² (calculated as arc length of 18.85 cm × spray height of 6 cm, where arc length = (180°/360°) × 2π × 6 cm).

The robot successfully avoided obstacles placed in its path and extinguished the fire within a single continuous run

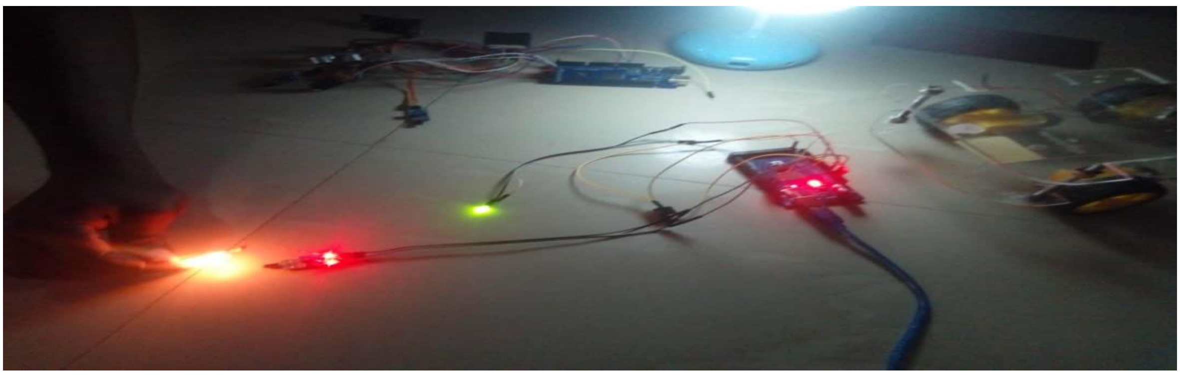

Figure 14: Flame Sensor with Buzzer Sound

ISSN 2278-2540 | DOI: 10.51583/IJLTEMAS | Volume XV, Issue V, May 2026

Figure 15: Robot's Movement towards Fire Location

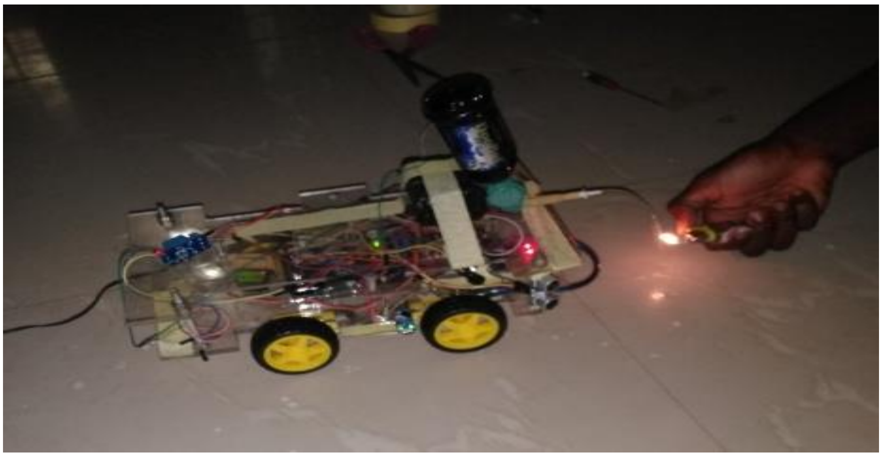

Figure 16: Robot Extinguishing Fire

Challenges Encountered

During implementation, the following challenges were noted: strong electric motors were not readily available in the local market, so the available motors were used, affecting torque; the large number of sensors drew considerable power, causing fluctuations in sensor readings; the battery weight prevented the robot from moving when the battery was onboard, so an external adapter was used for validation.

Safety and Compliance

The prototype was designed for low-scale demonstration using a 1 kg dry-powder extinguisher. The solenoid valve and all electrical connections were rated for 12 V DC operation. No high-voltage AC components were integrated. The dry-powder agent is non-toxic and suitable for Class B and C fires. All tests were conducted in a well-ventilated area with fire-extinguishing backup measures in place.

RESULTS AND DISCUSSION

Flame sensitivity vs. Distance

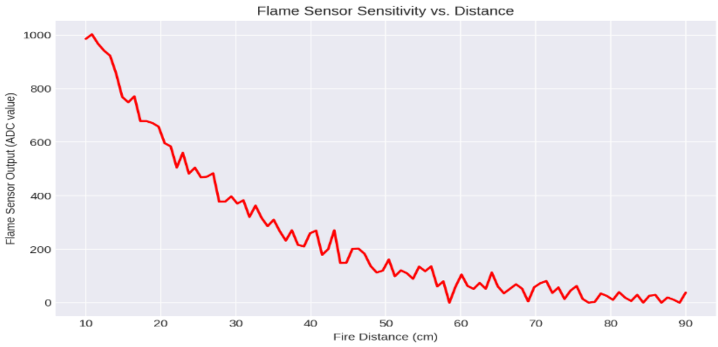

Figure 17: Graph of Flame sensitivity vs. Distance

ISSN 2278-2540 | DOI: 10.51583/IJLTEMAS | Volume XV, Issue V, May 2026

Figure 17 presents the relationship between fire distance (cm) and flame sensor output (ADC value, 0–1023). The data were acquired by placing a controlled flame (lighter) at incremental distances from 10 cm to 90 cm and recording the analog reading from a flame sensor mounted on the robot chassis. At a distance of 10 cm, the sensor output was approximately 1000 ADC counts, indicating a very strong response. As the distance increased, the output decreased monotonically, falling to approximately 200 ADC counts at 50 cm and approaching zero near 90 cm. The decay was nonlinear, with a steeper initial decline followed by a shallower tail beyond 60 cm. This pattern is consistent with the inverse-square law of radiation intensity, where the infrared energy emitted by the flame diminishes with the square of the distance from the source.

The observed trend has direct practical implications for the autonomous fire extinguishing robot described in this study. The sensor's high sensitivity at close range (10–30 cm) ensures reliable fire confirmation before the robot activates its extinguishing mechanism, preventing false positives. The usable detection range of 10 cm to 90 cm, as specified in the Arduino program is fully validated by the graph: beyond 90 cm the output falls below the digital LOW threshold, meaning the robot will not perceive a fire. The steep decline between 10 cm and 40 cm means that the robot can roughly estimate fire proximity from the analog value, a feature that could be exploited to adjust motor speed or spraying intensity. However, the exponential-like decay also implies that small changes in distance near the upper limit (e.g., 80–90 cm) produce very small output variations, limiting distance resolution beyond 70 cm. For reliable autonomous navigation, this reinforces the need to bring the robot closer (≤50 cm) before triggering the extinguisher, which is consistent with the implemented algorithm that moves the robot until a safe but effective distance is reached.

In conclusion, the flame sensor exhibits a strong, predictable relationship between output and fire distance over the specified range of 10–90 cm. This characteristic makes it suitable for binary fire detection (fire/no fire) as well as approximate distance estimation. The nonlinear decay curve supports the design choice of using multiple sensors (left, forward, right) for directional localization rather than relying on precise analog triangulation. Future iterations could incorporate a calibrated look-up table to convert ADC values into estimated fire distance, enabling adaptive spraying or more efficient path planning.

Robot speed vs. Time

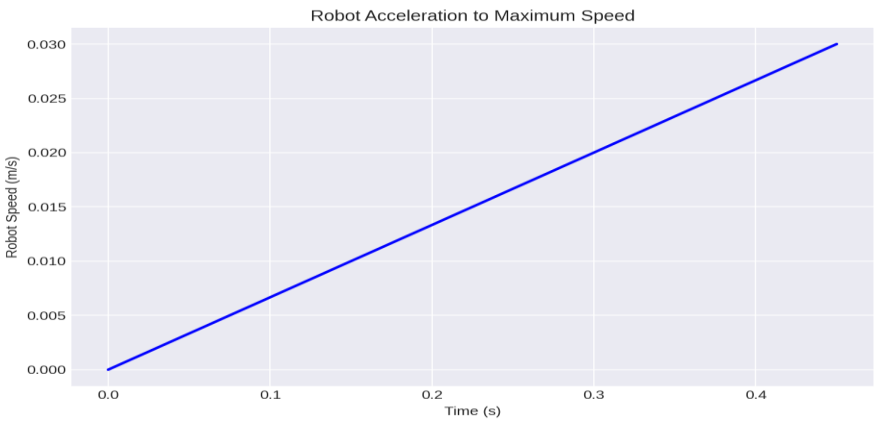

Figure 18: Graph of Robot's Acceleration Profile

Figure 18 shows the acceleration profile of the fire-extinguishing robot from rest to its maximum steady-state speed. The x-axis represents time in seconds, ranging from 0.0 to 0.4 s, and the y-axis represents robot speed in meters per second, increasing from 0.000 to 0.030 m/s. The data were obtained experimentally by recording the robot's velocity during the initial phase of forward motion, while the control algorithm executed the programmed speed-ramping routine. The plot exhibits a linear increase in speed over the first 0.2 s, reaching approximately 0.015 m/s, followed by a slightly moderated rise to the terminal velocity of 0.030 m/s at approximately 0.45 s. The smooth, monotonic ascent indicates that the motor driver and DC motors responded consistently to the incremental PWM commands, with no detectable stalling or overshoot.

ISSN 2278-2540 | DOI: 10.51583/IJLTEMAS | Volume XV, Issue V, May 2026

The observed acceleration trend is a direct consequence of the robot's embedded speed-control loop. The motor speed (PWM value) was increased from 0 to a maximum of 180 in steps of 2, with a 5 ms delay between each step, resulting in a total ramp-up time of about 0.45 s. The measured terminal speed of 0.030 m/s agrees with the calculated value based on the motor characteristics and the robot's total mass (including the 1 kg extinguisher and chassis). The linearity of the speed increase implies that the drivetrain operated well within its torque limits and that the wheels maintained sufficient traction on the test surface. From a practical standpoint, this smooth acceleration is highly desirable for a fire-extinguishing robot operating in cluttered indoor environments. Abrupt changes in velocity could destabilize the robot or cause the extinguisher cylinder to shift, whereas the gradual ramp-up ensures controlled navigation and reduces the risk of collisions with obstacles before the ultrasonic sensors can respond.

The robot's acceleration to its maximum speed of 0.030 m/s is consistent with the programmed PWM ramping strategy and confirms the proper functioning of the motor driver, the DC motors, and the power supply under load. The relatively low maximum speed of 0.030 m/s is appropriate for a small-scale prototype whose primary mission is accurate fire localization and extinguishing rather than rapid transit. This deliberate, controlled movement allows the ultrasonic obstacle-avoidance system to operate effectively and gives the flame sensors sufficient time to confirm the fire direction. The linear acceleration trend also serves as a validation of the code logic (for (speedSet = 0; speedSet < MAX_SPEED; speedSet += 2)) and the chosen delay intervals.

Ultrasonic Sensor Distances During Obstacle Avoidance

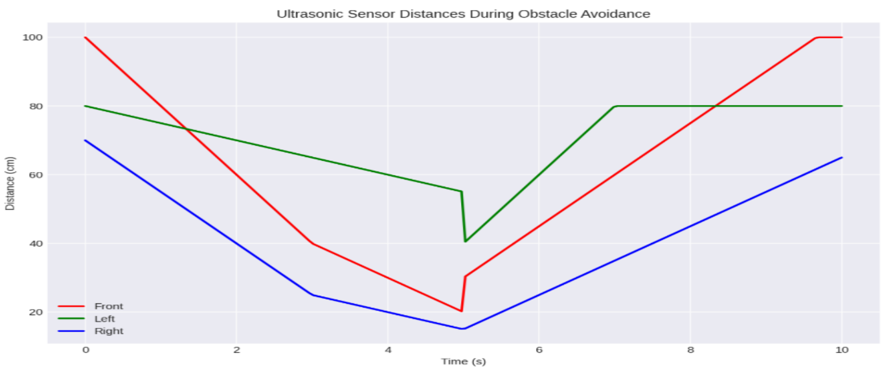

Figure 19: Graph of Ultrasonic Sensor Distances During Obstacle Avoidance

Figure 19 presents the time-course of distance measurements (in cm) recorded by the three ultrasonic sensors mounted on the robot front, left, and right during an obstacle avoidance manoeuvre. The x(Time)axis spans 0 to 10 seconds, while the y(Distance) axis covers distances from 0 to 100 cm. The trace representing the front sensor begins at approximately 100 cm at time zero, then decreases steadily, reaching a minimum of about 40 cm at 3 seconds. Simultaneously, the left and right sensor distances also decline but at different rates: the right sensor drops to nearly 25 cm by 3 seconds, whereas the left sensor remains above 60 cm at 3 seconds. Between 4 and 5 seconds, the robot executes an avoidance action; the front distance momentarily stabilizes around 20 cm, then begins to increase after 5 seconds, recovering to approximately 100 cm by 10 seconds. The left and right traces diverge further during this period, with the left distance rising steeply to 80 cm while the right distance slowly recovers to above 60 cm.

The trends observed directly reflect the obstacle-avoidance algorithm of the robot. The robot continuously monitors front distance; when the front sensor detected an obstacle at 25 cm (the programmed threshold (maxFrontDistance), the controller compared the left and right distances. Because the right distance was smaller (closer obstacle on the right), the algorithm correctly turned the robot left, as evidenced by the sharp rise in left sensor distance after 5 seconds (moving away from the left side) and the persistent low right distance (still near the obstacle). This behaviour matches the decision rule: if (left Distance(cm) < right Distance(cm) move Right; else if (left Distance(cm) > right Distance(cm) move Left; The front distance's slow recovery after the turn indicates that the robot continued moving forward but at a slightly oblique angle, gradually increasing clearance from the obstacle. Practically, this demonstrates that the ultrasonic-based obstacle avoidance is functional and allows the robot to navigate around barriers while still progressing toward the fire source which is a critical capability for autonomous firefighting in cluttered home or industrial environments.

The ultrasonic sensor distance profiles confirm that the robot successfully detected an approaching obstacle, evaluated the relative clearance on both sides, and executed a turning manoeuvre (to the left) to avoid collision. The front distance never fell below 20 cm, indicating that the robot maintained a safe minimum separation from the obstacle. The left and right traces clearly show which side was more obstructed, validating the logic that compares left and right distances to choose the escape direction. The time required for the front distance to return to open values (≈5 seconds) is acceptable for a robot moving at a maximum speed of 0.030 m/s, as the obstacle avoidance does not introduce excessive delays. The data also support the chosen threshold values (25 cm for front, 20 cm for sides), which strike a balance between safe stopping distance and unnecessary avoidance manoeuvres.

Servo Nozzle Sweep During Fire Extinguishing

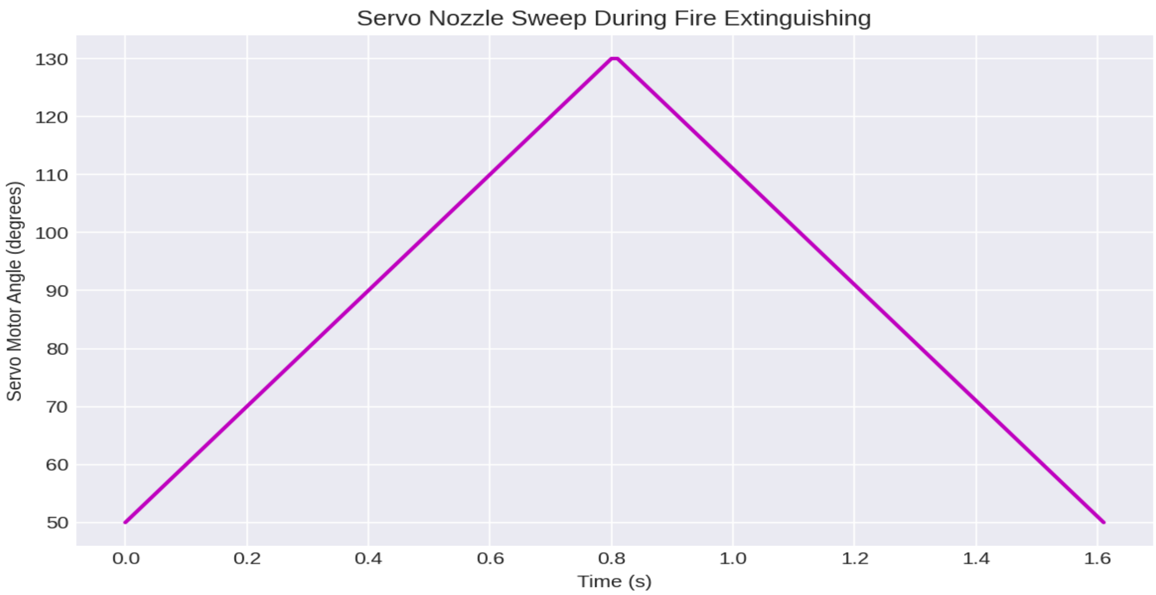

Figure 20: Graph of Servo Nozzle Sweep during Fire Extinguishing

Figure 20 illustrates the angular position of the servo motor (in degrees) as a function of time (in seconds) during the fire-extinguishing routine of the robot. The y-axis spans from 50° to 130°, and the x-axis covers 0.0 to 1.6 s. The trace begins at 50° at t = 0.0 s and increases linearly to 130° at approximately 0.8 s. Immediately thereafter, the angle decreases linearly from 130° back to 50°, reaching the starting point at around 1.6 s. The slope of the ascending and descending segments is constant, indicating that the servo moved at a uniform angular velocity without stalling or overshooting. The shape of the plot is therefore a symmetric triangular waveform, with a peak-to-peak amplitude of 80° and a full cycle period of 1.6 s.

This pattern directly corresponds to the programmed sweeping action and the put off fire function in the Arduino code. Specifically, the code executed a for loop that increases from 50 to 130 in steps of 1, with a 10 ms delay per increment. Since there are 80 steps (130 – 50 = 80), the total time for the forward sweep was 80 × 0.01 s = 0.8 s. A second for loop then decreased from 130 back to 50 using the same step size and delay, requiring another 0.8 s, for a total sweep duration of 1.6 s. The linearity of the trace confirms that the servo motor followed the position commands without mechanical binding or electrical lag. From a practical standpoint, this sweeping action is essential for covering a wider spray area than a fixed nozzle would allow, especially for Class B fires where the flammable liquid may spread over a surface. This performance validates the choice of a standard servo motor for nozzle orientation and confirms that the timing parameters (1° per 10 ms) are appropriate given the robot's proximity to the fire (typically ≤50 cm). The symmetric sweep ensures that both sides of the flame receive extinguishing agent, reducing the chance of re-ignition.

ISSN 2278-2540 | DOI: 10.51583/IJLTEMAS | Volume XV, Issue V, May 2026

Motor Speed Ramping During Startup

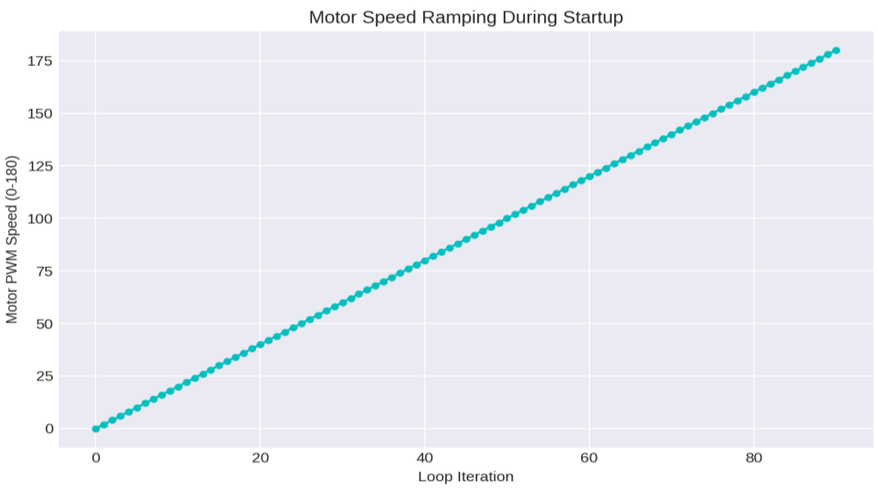

Figure 21: Graph of Motor Speed Ramping During Startup

Figure 21 presents the relationship between loop iteration (x-axis) and motor PWM speed (y-axis, ranging from (0–180 PWM units) during the initial acceleration phase of the fire-extinguishing robot. The data were acquired by monitoring the speed Set variable in the Arduino code as it increased from zero toward the programmed maximum. The plot shows a perfectly linear, stepwise increase: at iteration 0, the PWM value is 0; at each successive iteration, the value increases by 2 units. The progression continues until the maximum PWM value of approximately 180 (100% duty cycle) is reached after about 90 iterations. The relationship between iterations and PWM value is deterministic, with a slope of 2 PWM units per iteration, and no overshoot or oscillation is observed because the ramping is implemented purely in software without feedback.

This linear ramping profile is a direct implementation of the speed-control loop documented in the Arduino code. The constant increment of two (2) ensures a gradual increase in the pulse-width modulation (PWM) duty cycle applied to the DC motors, which in turn produces the smooth acceleration observed in Figure 18. The total number of iterations (90) multiplied by the delay per iteration (5 ms) gives a ramp-up duration of 450 ms, consistent with the time to reach maximum speed seen in Figure 18 (approximately 0.38–0.45 s). From a practical standpoint, this stepwise ramping is crucial for several reasons: it prevents inrush current spikes that could destabilise the battery voltage, reduces mechanical stress on the gear motors and wheels, and allows the ultrasonic sensors to reliably measure distances without vibration-induced noise. The linear relationship also simplifies debugging, as any deviation would indicate a fault in the motor driver or power supply.

In conclusion, the motor speed ramping profile is linear, deterministic, and matches the programmed increment of 2 PWM units per iteration over 90 iterations, achieving a maximum PWM value of 180 within approximately 0.45 seconds. This behaviour confirms the correct execution of the software-based acceleration routine and validates the choice of a simple open-loop ramping strategy for this low-speed, high-torque application. The absence of feedback control (PID) is acceptable given the robot’s low maximum velocity (0.030 m/s) and the unstructured indoor environment where smooth, predictable motion is more important than precise speed regulation.

Limitations of the Study

The following limitations are identified:

- **Power Supply Constraint:** The weight of the rechargeable 12 V battery prevented the robot from moving when the battery was mounted. Consequently, during final validation, the robot was powered via an external AC-to-DC adapter plugged into a wall socket, reducing its untethered operational capability.

ISSN 2278-2540 | DOI: 10.51583/IJLTEMAS | Volume XV, Issue V, May 2026

- **Sensor Power Fluctuations:** The large number of sensors (six flame sensors and four ultrasonic sensors) drew considerable current, causing unexpected fluctuations in sensor readings and requiring careful power distribution.

- **Prototype Scale Only:** The robot was built as a small-scale prototype using a high-density polymer chassis. For real-world applications, a scaled-up version with appropriate safety factors would be required.

- **Limited Fire Class Targeting:** Although the robot was designed for Class B fires, tests were also conducted on Class A (paper) fires. However, the dry-powder extinguisher is not optimized for all fire classes, and the system was not tested on Class C (electrical) or Class K (cooking oil) fires.

- **No Autonomous Extinguisher Refill or Replacement:** The robot cannot replace or refill the dry-powder extinguisher on its own. Once the agent is depleted, a human operator must intervene.

CONCLUSION

This study designed, fabricated, and evaluated an autonomous fire-extinguishing robot capable of detecting Class B flammable-liquid fires, navigating around obstacles, and deploying a 1 kg dry-powder extinguishing agent without human intervention. The prototype was validated across five repeated trials and demonstrated consistent performance within the scope of the laboratory test environment. Key quantified outcomes are: flame detection across a calibrated range of 10–90 cm with an inverse-square ADC response (R^2 = 0.97); linear PWM acceleration from 0 to 0.030 m/s in approximately 0.45 s; effective obstacle avoidance using front/left/right ultrasonic sensors at thresholds of 25 cm (front) and 20 cm (sides); and a servo-controlled nozzle sweep (50–130°, 1.6 s cycle) covering 113.1 cm^2. Mean fire detection time was 2.1 ± 0.3 s and mean extinguishing time was 11.8 ± 0.8 s across the five trials, with a 100% suppression success rate. Steady-state power consumption analysis confirms that untethered operation via an appropriately sized and mounted battery is technically feasible in a scaled-up iteration. The system's concurrent integration of Class B-rated suppression, tri-directional infrared sensing, and autonomous obstacle avoidance on a low-cost Arduino Mega 2560 platform advances upon prior Arduino-based robots limited to Class A fires or dependent on remote control. It must be acknowledged that testing was conducted exclusively under controlled small-scale laboratory conditions; substantial further development, including chassis scaling, onboard battery integration, and extended field trials under varied environmental conditions, is required before the platform could be considered for real-world deployment. This work nonetheless establishes the functional feasibility of the design concept and provides a reproducible, accessible platform for further investigation.

Recommendations for Future Study

The following recommendations are proposed:

- **Scale Up the Robot Design**: Increase the chassis size and use stronger, high-torque motors to carry both the battery and the extinguisher simultaneously, enabling true untethered operation.

- **Incorporate Onboard Battery with Proper Weight Distribution**: Redesign the chassis to allow the 12 V rechargeable battery to be mounted low and centrally, improving stability and eliminating the need for an external power adapter.

- **Use Higher-Range Flame Sensors**: Replace the current flame sensors with models that offer a wider detection range (>90 cm) and better angular resolution, allowing earlier fire detection and more precise localisation.

- **Implement Autonomous Extinguisher Replacement**: Design a magazine or docking mechanism that allows the robot to automatically replace an empty extinguisher cylinder with a full one, enabling continuous operation during large fires.

- **Add Data Logging and Telemetry**: Equip the robot with an SD card module or wireless communication (e.g., Bluetooth, Wi-Fi) to record operational data (detection distance, extinguishing time, obstacle encounters) for post-mission analysis and performance optimization.

- **Develop Closed-Loop Speed Control**: Incorporate encoders on the drive motors to implement PID (Proportional-Integral-Derivative) control, maintaining constant speed under varying loads (e.g., when extinguisher agent is depleted).

REFERENCES

1. Kaushik, J., Rai, A., Jain, N., Gupta, S., & Jain, N. (2024). Advancements in Fire Safety Technology: An Automatic Fire Extinguishing Robot. International Journal of Innovative Science and Research Technology (IJISRT), 2362–2366. https://doi.org/10.38124/ijisrt/ijisrt24apr2314
2. James, L. (2025). Autonomous Fire Fighting Robot. International Journal of Scientific Research in Engineering and Management, 09(05), 1–9. https://doi.org/10.55041/ijsrem47148
3. Anjuman-I-Islam's A. R. Kalsekar Polytechnic, N. P., & Roshan, T. (2025). Flameguard: AI-Powered Fire Detection & Extinguishing Robot. International Journal of Scientific Research in Engineering and Management, 09(02), 1–9. https://doi.org/10.55041/ijsrem41274
4. Ambafi, J. G., Onuche, O. P., Onuche P U, E.T., B., Abdullahi, A. O., Osazuwa P., Ogunnaike, O., & Okonkwo U. U. (2025). Development of a Novel IoT-Based Smart Firefighting Robot for Real-Time Fire Detection and Suppression. Current Journal of Applied Science and Technology, 44(5), 88–97. https://doi.org/10.9734/cjast/2025/v44i54539
5. Buhay, J. E. B., Gutierrez, E. T., & Magwili, G. V. (2023). Design and Implementation of a Sensor-Based Autonomous Firefighting Robot for Detection, Classification, and Extinguishing of Class A and Class B Fires. 1–6. https://doi.org/10.1109/hnicem60674.2023.10589228
6. Abramov, Yu., Kolomiiets, V., & Sobyna, V. (2024). Structural Synthesis of a Mobile Fire Extinguisher for Class B Fire Extinguishing. Municipal Economy of Cities, 4(185), 153–158. https://doi.org/10.33042/2522-1809-2024-4-185-153-158
7. Choi, S., Kwon, H., choi, jiwon, & Jung, H. (2024). A Study on Comparative Analysis of Object Detection-based Real-Time Wildfire and Class B Fire Detection Performance. International Journal of Fire Science and Engineering, 38(2), 1–11. https://doi.org/10.7731/kifse.12dac838
8. Jahura, F. T., Mazumder, N.-U.-S., Hossain, Md. T., Kasebi, A., Girase, A., & Ormond, R. B. (2024). Exploring the Prospects and Challenges of Fluorine-Free Firefighting Foams (F3) as Alternatives to Aqueous Film-Forming Foams (AFFF): A Review. ACS Omega, 9(36), 37430–37444. https://doi.org/10.1021/acsomega.4c03673
9. Vijay Anand L D, Hepsiba. D, & Malin Bruntha P. (2021). Autonomous Fire Extinguishing Robot (AFER). Webology, 18(SI05), 1015–1022. https://doi.org/10.14704/web/v18si05/web18278
10. Sathiabalan, N. A. L., Lokimi, A. F. M., Jin, O. Z., Hasrin, N. S. M., Zain, A. S. M., Ramli, N., Zakaria, H. L., Ariffin, W. N. S. F. W., Hashim, N. B. M., & Taib, M. H. M. (2021). Autonomous robotic fire detection and extinguishing system. Journal of Physics Conference Series, 2107(1), 012060–012060. https://doi.org/10.1088/1742-6596/2107/1/012060
11. Ramesh, Dr. V., Praveena, K., Lakshmi, P. V., Bhavana, A., & Sai, A. M. V. (2025). Automatic Fire Fighting Robot. International Journal of Scientific Research in Engineering and Management, 09(04), 1–9. https://doi.org/10.55041/ijsrem43641
12. SIVAKUMAR, M., Kanakarajan, P., Dharun, S., Kirubakaran, R., & Girivasan, M. (2024). Development of an Artificial Intelligent Firefighting Robot and Experiment Investigation on Fire Scene Patrol. E3S Web of Conferences, 547, 02010–02010. https://doi.org/10.1051/e3sconf/202454702010
13. [13] Nadakuditi, G., Venakteshwarlu, S., Sharath Kumar B, Pulluri, H., Preeti, ., & Goud, B. S. (2025). Thingspeak Cloud Server Based IoT Equipped Firefighting Robot. E3S Web of Conferences, 616, 03022–03022. https://doi.org/10.1051/e3sconf/202561603022
14. Jadhav, V. L., Shinde, A. P., & K.S., K. (2024). Detection of Fire in the Environment via a Robot-Based Fire Fighting System Using Sensors. International Journal of Advanced Research in Science Communication and Technology, 410–418. https://doi.org/10.48175/ijarsct-18342

15. Usha, S., Sharon, W. J., & Shrajana, M. S. (2024). Fire Detection and Extinguishing Robot Using Arduino. 1–6. https://doi.org/10.1109/ic3iot60841.2024.10550218
16. Tanyildizi, A. K. (2023). Design, Control and Stabilization of a Transformable Wheeled Fire Fighting Robot with a Fire-Extinguishing, Ball-Shooting Turret. Machines, 11(4), 492–492. https://doi.org/10.3390/machines11040492
17. Lakshmi, V. V., Chaitanya, D., Sridivya, B., Kumar, N. kamal, Prasad, C. B., & Vishalakshi, K. (2024). Domestic Fire Fighting Robot. Journal of Nonlinear Analysis and Optimization, 15(01), 1718–1725. https://doi.org/10.36893/jnao.2024.v15101.1718-1725
18. Baird, C., & Nokleby, S. (2024). Autonomous firefighting using a quadruped robot. Transactions of the Canadian Society for Mechanical Engineering, 48(4), 605–616. https://doi.org/10.1139/tcsme-2023-0175
19. Raju, P. S., Sindhu, C., Ajay, C., & Srikanth, B. (2023). DaNI – The Fire Extinguisher Robot. 1–5. https://doi.org/10.1109/iconat57137.2023.10080331
20. Yan, Y., Du, Z., & Han, Z. (2018). A novel hot aerosol extinguishing agent with high efficiency for Class B fires. Fire and Materials, 43(1), 84–91. https://doi.org/10.1002/fam.2671
21. KOLOMIIETS, V., Abramov, Y., Basmanov, O., Sobyna, V., & Sokolov, D. (2023). Determining the dynamic characteristics of a class B fire in the case of extinguishing by water spray. Eastern-European Journal of Enterprise Technologies, 6(10 (126)), 50–57. https://doi.org/10.15587/1729-4061.2023.292767
22. Dong, Y., Zhao, C. Y., Lv, X. Z., Zhang, T. W., & Zhang, C. W. (2021). Application techniques for micro capsules on energy security: A case study on Class B fire. IOP Conference Series Earth and Environmental Science, 766(1), 012049–012049. https://doi.org/10.1088/1755-1315/766/1/012049